

An unexplored valley of binary packing: The loose jamming state

Si Suo^{1,2,3#}, Chongpu Zhai^{1#}, Minglong Xu^{1*}, Marc Kamlah², Yixiang Gan^{4,5**}

¹ *State Key Laboratory for Strength and Vibration of Mechanical Structures, School of Aerospace,*

Xi'an Jiaotong University, Xi'an, China

² *Institute for Applied Materials, Karlsruhe Institute of Technology (KIT), Germany*

³ *Department of Engineering Mechanics, FLOW Centre, KTH, Stockholm SE-100 44, Sweden*

⁴ *School of Civil Engineering, The University of Sydney, Sydney, NSW 2006, Australia*

⁵ *The University of Sydney Nano Institute (Sydney Nano), The University of Sydney, Sydney, NSW 2006,*

Australia

We present a theoretical prediction on random close packing factor ϕ_{RCP}^b of binary granular packings based on the hard-sphere fluid theory. An unexplored regime is unravelled, where the packing fraction ϕ_{RCP}^b is smaller than that of the mono-sized one ϕ_{RCP}^m , i.e., the so-called loose jamming state. This is against our common perception that binary packings should always reach a denser packing than mono-sized packings at the jamming state. Numerical evidence further supports this prediction and confirms the regime location in the size ratio and mole fraction (R_r - X_s) space, where the size ratio R_r is close to 1, and the mole fraction of the smaller sphere X_s close to 0. This extreme regime remains unreported in existing literature, yet significant for our fundamental understanding of binary packing systems.

Contribute equally.

* Corresponding author. Email: mlxu@mail.xjtu.edu.cn.

** Corresponding author. Email: yixiang.gan@sydney.edu.au

Introduction

The random close packing (RCP) problem has attracted extensive attention, which is of great importance not only in our exploration into the fundamental physics of glasses, liquids, colloidal systems [1], but also in facilitating optimisation of conveying, handling and processing different types of granular materials [2]. The RCP problem can be dated back to Bernal and Mason's experimental study on packings with identical spheres, in which the random close packing factor for mono-sized packing, ϕ_{RCP}^m , was measured to be around 0.64 with an average coordination number, Z_c^m , of 6 [3]. Following experimental and numerical studies [4-8] reported that ϕ_{RCP}^m generally ranges from 0.61 to 0.69. Despite great progress in both experimental and numerical studies [9-12], we still lack a comprehensive understanding of RCP, especially for binary packings, in terms of the particle-scale driving mechanism, collective behaviour of jamming development [13, 14], tuneable properties including stiffness, mechanical stability [6], anti-crystallization [15, 16], thermal and electrical conduction [17, 18].

Few analytical approaches have been reported enabling satisfactory interpretation for definition, formation, characterization of mono-sized RCP. These models [19-22] tend to simplify the structure evolution of RCP by concentrating on the contacting neighbours of an individual particle, while ignoring influences of non-contacting surrounding particles. Very recently, Zaccone [23] proposed a simple route towards an analytical value of ϕ_{RCP}^m using a nearest-neighbour statistics as well as respecting the known closest packing ($Z_c^m = 12$, $\phi_{CP}^m \approx 0.74$). Noticeably, no extra fitting parameters are required in this scheme and the predicted ϕ_{RCP}^m highly matches the measurements from existed experiments and simulations.

Regarding binary granular packings, the mixture can usually fill more space than that of mono-sized packings, with the corresponding RCP factor $\phi_{RCP}^b > \phi_{RCP}^m$. Theoretical solutions for both mono-sized packings [24] and binary mixtures [25] were developed based on equilibrium statistical mechanics. The current focus is on situations with moderate or extremely small size ratio R_r (small radius on large one) [10-12, 16, 26].

A quantity of empirical packing models were proposed based on the assumption that fine particles can fill the void among large particles [27-29]. However, the other near-boundary extreme region, i.e., $R_r \rightarrow 1$, has been seldom investigated, as an asymptotic trend to the mono-sized packing can be expected.

In this letter, we remedy to the unexplored region from theoretical and numerical aspects. Firstly, the Zacccone's scheme is extended to the binary packing problem, and at the near-boundary region the theoretical solution indicates an "abnormal" valley, where $\phi_{RCP}^b < \phi_{RCP}^m$, i.e., a so-called loose jamming state. Then, we further provide numerical evidence to support our theoretical prediction.

Theory

Here, the hard-sphere (HS) fluid theory is employed for estimating the partial radial distribution functions (RDF) in binary packing, allowing the statistical description of the local structure around a sphere. Specifically, three types of sphere-to-sphere interaction including small-small, large-large, and small-large pairs, with $g_{ss}(d)$, $g_{ll}(d)$ and $g_{sl}(d)$, respectively, indicate the probability density within a radial distance of d . Correspondingly, the contact value $Z_{c,ij}$ for the above three pair types (i, j for s or l) can be given by [23]

$$Z_{c,ij} = 4\pi\rho \int_0^{d_{ij}+\varepsilon} g_{ij}^0 g_{ij}(d_{ij})\delta(r - d_{ij})r^2 dr, \quad (1)$$

where d_{ij} is the centre distance between two contacting spheres; ρ is the number density, i.e. $\rho = (N_s + N_l)/V$ with N_s and N_l being the number of small and large spheres within a volume of V ; g_{ij}^0 is a factor to be determined from the consistency conditions stated later. By weighting the contact value with mole fraction, the average coordination number Z_c^b of a binary packing is

$$Z_c^b(X_s, R_r) = X_s(Z_{c,ss} + Z_{c,sl}) + X_l(Z_{c,ll} + Z_{c,ls}), \quad (2)$$

where the mole fraction $X_i = N_i/(N_s + N_l)$ and the size ratio $R_r = d_s/d_l$. Naturally, the binary packing reduces to mono-sized packing, i.e., $Z_c^b(X_s, R_r)$ should be consistent with Z_c^m under the following situations, i.e., the so-called consistency conditions:

$$Z_c^b(0, R_r) = Z_c^m; Z_c^b(1, R_r) = Z_c^m; Z_c^b(X_s, 1) = Z_c^m. \quad (3)$$

Moreover, substituting Eq. (1) into Eq. (2), Z_c^b reads

$$Z_c^b = 4\pi\rho g^0 [X_s d_s^3 \tilde{g}_{ss}^0 g_{ss}(d_{ss}) + X_l d_l^3 \tilde{g}_{ll}^0 g_{ll}(d_{ll}) + d_{sl}^3 \tilde{g}_{sl}^0 g_{sl}(d_{sl})], \quad (4)$$

where the factor g_{ij}^0 of Eq. (1) is expressed as $g_{ij}^0 = g^0 \tilde{g}_{ij}^0$. Here, g^0 is a normalization constant, and as followed by Zaccone's route [23], g^0 can be determined by introducing the conclusion of the mono-sized close packing ($Z_c^m = 12$, $\phi_{CP}^m \approx 0.74$); \tilde{g}_{ij}^0 is responsible for the consistency condition and therefore it is a function of X_s and normalized within $[0, 1]$. Specifically, corresponding to the consistency conditions, the constraints on \tilde{g}_{ij}^0 are given respectively by

$$\tilde{g}_{ss}^0(0) = 0; \tilde{g}_{ss}^0(1) = 1; \quad (5)$$

$$\tilde{g}_{ll}^0(0) = 1; \tilde{g}_{ll}^0(1) = 0; \quad (6)$$

$$X_s \tilde{g}_{ss}^0(X_s) + (1 - X_s) \tilde{g}_{ll}^0(X_s) + \tilde{g}_{sl}^0(X_s) = 1. \quad (7)$$

Under the constraints of Eqs. (5)~(7), the possible format of \tilde{g}_{ij}^0 can be

$$\tilde{g}_{ss}^0(X_s) = X_s; \tilde{g}_{ll}^0(X_s) = 1 - X_s; \tilde{g}_{sl}^0(X_s) = 2X_s(1 - X_s). \quad (8)$$

Regarding $g_{ij}(d_{ij})$, the theory on additive HS mixtures, as an extension of the mono-component one, can provide a statistical solution, e.g., the BMCSL scheme [30] extended from the Carnahan-Starling equation [31]. It has been proved that the estimation on $g_{ij}(d_{ij})$ given by the original BMCSL expression is remarkably accurate for the moderate region of X_s and R_r , while for regions $X_s \rightarrow 0$ or $X_s \rightarrow 1$ of interest in this work, deviation occurs [32, 33]. Thus, we employ a modified version which improved the BMCSL expression to fully satisfy the nine consistency conditions for binary mixtures by adding an additional term [33]. Moreover, in order to generate a quantitative description and better agree with the experimental and simulation results, two adjustable indexes n_l and n_s are introduced on the additional term whilst all consistency conditions in [33] are respected. The final expressions, where $g_{ij}^{\text{BMCSL}}(d_{ij})$ is the contact value of the RDF from the BMCSL expression, explicitly read

$$g_{ll}(d_{ll}) = g_{ll}^{\text{BMCSL}}(d_{ll}) + \left(\frac{X_s}{4} \frac{\xi_1 \xi_2}{(1 - \xi_3)^2} \frac{d_{ll} - d_{ss}}{d_{sl}} d_{ll}^2 d_{ss} \right)^{n_l}, \quad (9)$$

$$g_{ss}(d_{ss}) = g_{ss}^{\text{BMCSL}}(d_{ss}) + \left(\frac{X_l}{4} \frac{\xi_1 \xi_2}{(1-\xi_3)^2} \frac{d_{ll}-d_{ss}}{d_{sl}} d_{ss}^2 d_{ll} \right)^{n_s}, \quad (10)$$

$$g_{sl}(d_{sl}) = g_{sl}^{\text{BMCSL}}(d_{sl}) + \left(\frac{1}{4} \frac{\xi_1 \xi_2}{(1-\xi_3)^2} \frac{d_{ll}-d_{ss}}{d_{sl}} \frac{d_{ll} d_{ss}^3}{d_{sl}} \right), \text{ and} \quad (11)$$

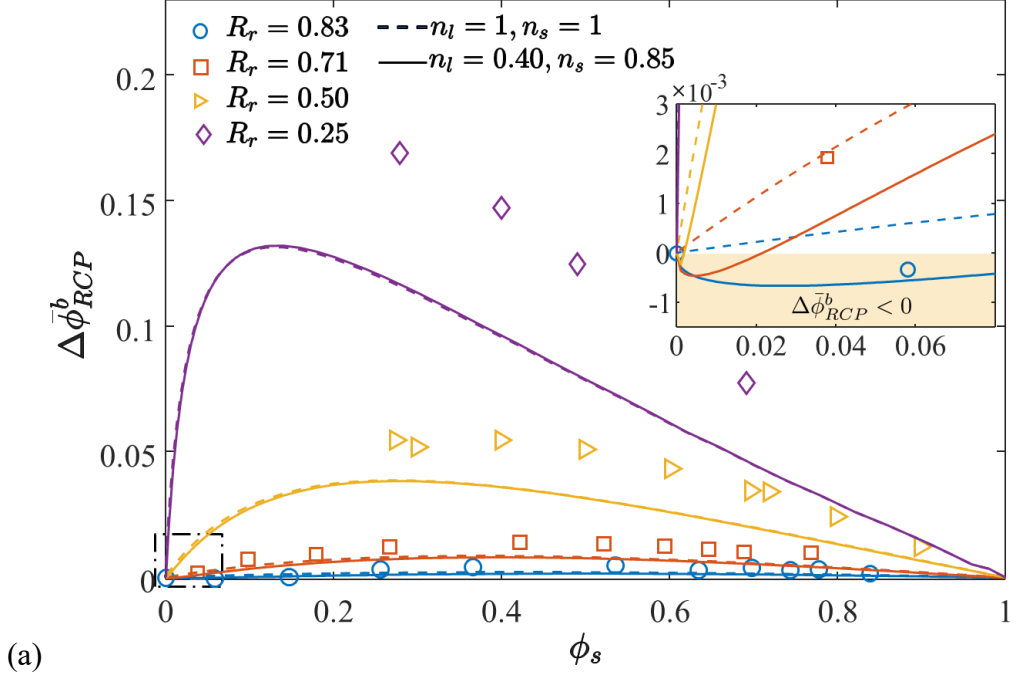
$$\xi_n = \frac{\pi}{6} \rho \sum_i x_i d_{ii}^n. \quad (12)$$

In the original BMCSL scheme [24], both n_l and n_s equal 1. Alternative modifications based on the BMCSL scheme can be referred to [34, 35]. However, they can not output better predictions than Eq. (9)~(12).

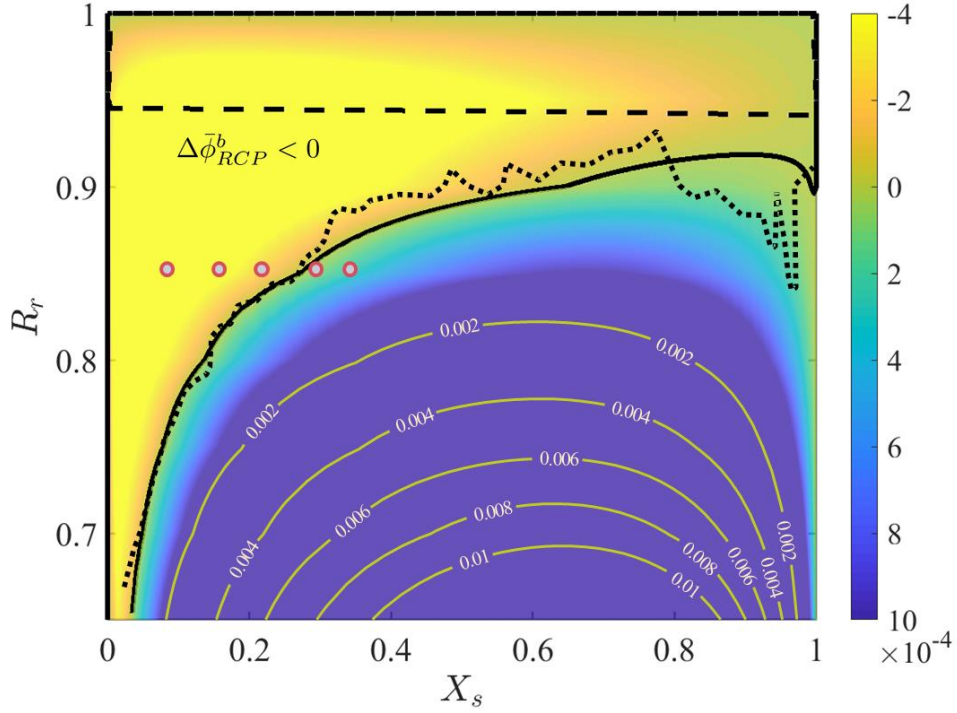
Substituting Eqs. (9)~(11) into Eq. (4) and setting $Z_c^b = 6$ establish an equation regarding ϕ_{RCP}^b , X_s and R_r , and thus we can solve ϕ_{RCP}^b on the R_r - X_s space. To better demonstrate the tendency of ϕ_{RCP}^b with R_r and X_s , and further emphasize the comparison between ϕ_{RCP}^b and ϕ_{RCP}^m , we introduce a relative value $\Delta\bar{\phi}_{RCP}^b$ to describe the difference as,

$$\Delta\bar{\phi}_{RCP}^b = \frac{\phi_{RCP}^b - \phi_{RCP}^m}{\phi_{RCP}^m}. \quad (13)$$

We firstly solve the distribution of ϕ_{RCP}^b based on the original expression in [33], i.e., $n_l = 1$ and $n_s = 1$, and compare our prediction against the reported data in [25]. As shown in Figure 1(a), the prediction of our theory can capture the tendency of ϕ_{RCP}^b , i.e., an asymmetric distribution along X_s , which is also in agreement with direct observations from other experiments and simulations [12, 16, 36]. Furthermore, the solution quantitatively matches the reported data in the region $R_r \rightarrow 1$, though an obvious deviation is observed in the moderate- R_r region ($R_r < 0.5$). This drawback is likely to be conquered by trying other statistical models, such as Percus-Yevick theory [37] and the Carnahan-Starling equation [31]. However, we stick to the current scheme since its solution is accurate enough for the region of our interest. More important, the obtained theoretical results predict a valley region ($\Delta\bar{\phi}_{RCP}^b < 0$) near the boundaries ($R_r = 1$ and $X_s = 0$), as highlighted by the black dash lines in Figure 1(b), constituting the so-called loose jamming state. To further confirm the existence of this valley region, numerical evidence is provided below.



(a)



(b)

Figure 1. (a) Relative packing factor $\Delta\bar{\phi}_{RCP}^b$ vs. volume fraction of the small component, $\phi_s = X_s R_r^3 / (X_s R_r^3 + X_l)$. Open symbols are data reported in [25]; dash lines are theoretical prediction base on the Eqs. (9)~(11) with $n_l = 1$ and $n_s = 1$ while solid lines are the one with $n_l = 0.40$ and $n_s = 0.85$. The subfigure is a zoom-in view of near-boundary region ($X_s \rightarrow 0$). (b) The contour plot of the relative packing factor $\Delta\bar{\phi}_{RCP}^b$ from simulations on the R_r - X_s space. The valley region appears in yellow. The

dashed line represents the prediction by the original expression of $g_{ij}(d_{ij})$ in [33], with $n_l = 1$ and $n_s = 1$; the dotted line is extracted from simulation results; the solid line is predicted by Eqs. (9)~(11) with $n_l = 0.40$ and $n_s = 0.85$, selected for fitting the simulation data. Symbol \circ can be referred to Figure 2 for further statistical analyses of the local packing structure of spheres.

Simulations

Numerical simulations are performed by an inhouse code, KIT-DEM [18, 38]. Each configuration is identified by a unique size ratio R_r and mole fraction X_s , and is repeated for five samples. Each packing contains 5000 frictionless non-cohesive spherical particles which are randomly packed within a periodic cubic domain as an initial state [39]. The Hertzian contact model is adopted and the elasticity modulus is set large enough to guarantee the final particle-particle overlap is smaller than 0.1% particle radius so that the hard-sphere assumption can be satisfied. All packings are uniaxially compressed using a quasi-static protocol [38] until reaching the jamming point where the average coordination number Z_c increases to six and the increment rate of Z_c starts to demonstrate a sharp decay [12]. The critical packing factor is then obtained at the jamming point, and for each configuration ϕ_{RCP} is calculated as the mean value over its five repeated cases, and the standard deviation at the valley is 1.3×10^{-4} while the corresponding $\Delta\bar{\phi}_{RCP}^b = -1.7 \times 10^{-3}$.

Results and Discussion

The relative packing factor $\Delta\bar{\phi}_{RCP}^b$ with respect to R_r and X_s extracted from the conducted simulations is plotted in Figure 1(b). The introduced indexes n_l and n_s in Eqs. (9) and (10) are adjusted to ensure that the theoretical solution matches simulation results, and a good agreement can be obtained when $n_s = 0.40$ and $n_l = 0.85$, as shown in Figure 1(b) where the original expression in [24] (with $n_l = 1$ and $n_s = 1$), is also included to compare with the simulation results. To be safe, we also test this modified version against the original version and the reported data. In Figure 1(a),

solutions based on the different groups of n_l and n_s are almost the same over the most range of ϕ_s , except in the range of $\phi_s \rightarrow 0$, see the subfigure. This suggests that modifying the additional terms in Eqs. (9) and (10) can only effectively influence the near-boundary range rather than the moderate R_r - X_s space. Moreover, the proposed expression with modified n_l and n_s is capable of predicting the loose jamming region, which is not only confirmed by our simulation results but also supported by the data reported in [25] on a qualitative basis.

In addition to the statistical view on the binary packing and its loose jamming state, we further provide a meso-scale insight into this unexplored valley with the help of the pair correlation function $p(r)$ [40, 41], which can measure the probability density of possible distances between centres of two particles (\vec{c}_i and \vec{c}_j) within a radial space, and thus it is defined as

$$p(r) = \frac{1}{\rho(N_s+N_l)} \sum_{\vec{c}_i} \sum_{\vec{c}_j} \delta[(|\vec{c}_i - \vec{c}_j| - r) \cdot (r + b - |\vec{c}_i - \vec{c}_j|)] \frac{1}{4\pi r^2 b}. \quad (14)$$

The peak value of $p(r)$ occurs corresponding to a certain particle-particle configuration, which is classified into three neighbouring layers (not limited to three, but the most related ones are discussed here). Figure 2 (a)~(e) demonstrate a transition from the loose to normal jamming state. From the variation of $p(r)$ with X_s , the third peak moves leftwards from $2.65d_l$, where large particles dominate the third layer, to smaller than $2.56d_l$, suggesting small particles break through the third layer into the second. In other words, the jamming state turns to normal (with the third peak of $2.65d_l$ in $p(r)$) from the loose one (with the third peak of $2.56d_l$ in $p(r)$) as we increase the amount of small spheres in the mixture, illustrated in Figure 2(f). Additionally, the second peak becomes obscure even vanishes after the jamming state transition, see (d) and (e), indicating small particles contribute more to the second and third peaks in $p(r)$, and even dominating the third layer. Therefore, the impact of small particles on the third layer can be regarded as a meso-scale judgement on the jamming state, and the critical position of third peak on $p(r)$ defines the phase boundary.

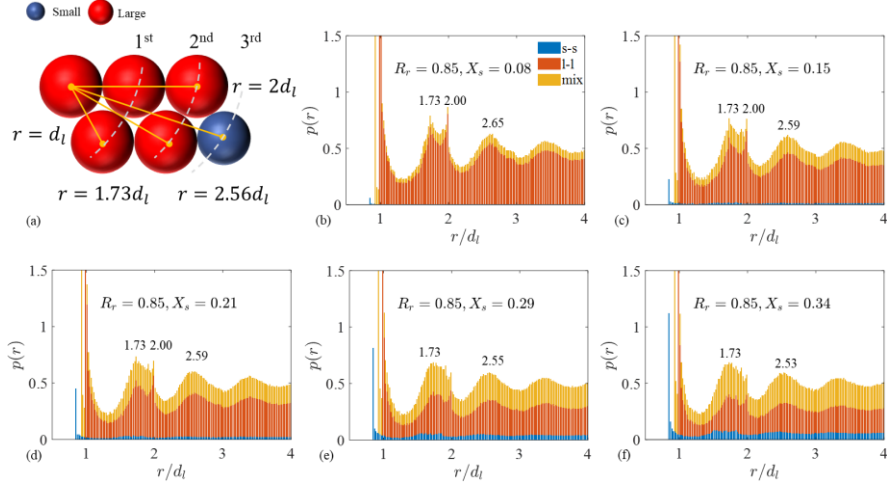


Figure 2. The variation of pair correlation function $p(r)$ of $R_r = 0.85$ crossing the border of loose jamming state with increasing X_s , i.e., from (b-d) locating within the valley region to (e-f) locating outside, and the corresponding positions on the R_r - X_s space can be referred to the symbol \odot in Figure 1(b). The values of r/d_l at the local peaks of $p(r)$ are indicated, and can be referred to the particle-particle topology in (a).

Conclusions

In this letter, we have developed a theoretical model by extending the recent Zaccone's scheme [23] for predicting the RCP of binary granular assemblies. The proposed model has been firstly validated against the data reported in [25] focusing on the relationship between the packing factor and volume fraction of small spheres. The analytical solution predicts an unexpected valley region on R_r - X_s space, i.e., the loose jamming state, at which ϕ_{RCP}^b is smaller than ϕ_{RCP}^m against the common observation within the moderate R_r - X_s range that ϕ_{RCP}^b should be always larger than ϕ_{RCP}^m . Subsequently, this valley indicating the phase transition from loose to normal jamming states has been further confirmed through DEM simulations and the exact phase boundary of the loose jamming state is established. The simulation data also provided a meso-scale insight into this observed transition with increasing fraction of smaller particles, during which small particles gradually dominate the third layer and are mixed into the second layer. Finally, we linked the statistical description of the loose jamming

state with a meso-scale explanation based on particle-particle topology.

In the future, this theoretical approach can be possibly extended to polydisperse granular media. Compared with the binary packing, it seems likely to realize much looser jamming packings by adjusting size distribution. Since mechanical and transport properties of granular materials are related to packing structures, this adjustable jamming state may lead to important engineering practices, such as lightweight concrete design [42], microstructure design of battery electrodes[43], and optimized granular beds for water retention [44, 45], filtration [46, 47], and thermal energy storage [48, 49].

This work was supported by State Key Laboratory for Strength and Vibration of Mechanical Structures under SV2021-KF-27.

1. Annabattula, R.K., Y. Gan, and M. Kamlah, *Mechanics of binary and polydisperse spherical pebble assembly*. Fusion Engineering and Design, 2012. **87**(5): p. 853-858.
2. Oda, M. and K.e. Iwashita, *Mechanics of granular materials: an introduction*. 2020: CRC press.
3. Bernal, J.D. and J. Mason, *Packing of Spheres: Co-ordination of Randomly Packed Spheres*. Nature, 1960. **188**(4754): p. 910-911.
4. Jodrey, W.S. and E.M. Tory, *Computer simulation of close random packing of equal spheres*. Physical Review A, 1985. **32**(4): p. 2347-2351.
5. Berryman, J.G., *Random close packing of hard spheres and disks*. Physical Review A, 1983. **27**(2): p. 1053-1061.
6. Torquato, S., T.M. Truskett, and P.G. Debenedetti, *Is random close packing of spheres well defined?* Physical review letters, 2000. **84**(10): p. 2064.
7. Zinchenko, A.Z., *Algorithm for Random Close Packing of Spheres with Periodic Boundary Conditions*. Journal of Computational Physics, 1994. **114**(2): p. 298-307.
8. Scott, G.D. and D.M. Kilgour, *The density of random close packing of spheres*. Journal of Physics D: Applied Physics, 1969. **2**(6): p. 863-866.
9. Desmond, K.W. and E.R. Weeks, *Random close packing of disks and spheres in confined geometries*. Physical Review E, 2009. **80**(5): p. 051305.
10. Pillitteri, S., et al., *From jamming to fast compaction dynamics in granular binary mixtures*. Scientific Reports, 2019. **9**(1): p. 7281.
11. Prasad, I., C. Santangelo, and G. Grason, *Subjamming transition in binary sphere mixtures*. Physical Review E, 2017. **96**(5): p. 052905.
12. Petit, J.C., et al., *Additional Transition Line in Jammed Asymmetric Bidisperse Granular Packings*. Physical Review Letters, 2020. **125**(21).
13. Behringer, R.P. and B. Chakraborty, *The physics of jamming for granular materials: a review*. Reports on Progress in Physics, 2018. **82**(1): p. 012601.
14. Ottino, J.M. and D.V. Khakhar, *Mixing and Segregation of Granular Materials*. Annual Review of Fluid Mechanics, 2000. **32**(1): p. 55-91.
15. Kumar, N., et al., *Tuning the bulk properties of bidisperse granular mixtures by small amount of fines*. Powder Technology, 2016. **293**: p. 94-112.
16. Pillitteri, S., et al., *How size ratio and segregation affect the packing of binary granular mixtures*. Soft Matter, 2020. **16**(39): p. 9094-9100.
17. Zhai, C., et al., *Stress-dependent electrical transport and its universal scaling in granular materials*. Extreme Mechanics Letters, 2018. **22**: p. 83-88.
18. Suo, S., et al., *Cyclic thermo-mechanical performance of granular beds: Effect of elastoplasticity*. Powder Technology, 2021.
19. Song, C., P. Wang, and H.A. Makse, *A phase diagram for jammed matter*. Nature, 2008. **453**(7195): p. 629-632.
20. Kamien, R.D. and A.J. Liu, *Why is Random Close Packing Reproducible?* Physical Review Letters, 2007. **99**(15): p. 155501.
21. Dodds, J.A., *Simplest statistical geometric model of the simplest version of the multicomponent random packing problem*. Nature, 1975. **256**(5514): p. 187-189.
22. Ouchiyama, N. and T. Tanaka, *Porosity of a mass of solid particles having a range of sizes*. Industrial & Engineering Chemistry Fundamentals, 1981. **20**(1): p. 66-71.

23. Zaccone, A., *Explicit Analytical Solution for Random Close Packing in $d=2$ and $d=3$* . Physical Review Letters, 2022. **128**(2): p. 028002.
24. Parisi, G. and F. Zamponi, *The ideal glass transition of hard spheres*. The Journal of Chemical Physics, 2005. **123**(14): p. 144501.
25. Biazzo, I., et al., *Theory of Amorphous Packings of Binary Mixtures of Hard Spheres*. Physical Review Letters, 2009. **102**(19): p. 195701.
26. Srivastava, I., et al., *Jamming of bidisperse frictional spheres*. Physical Review Research, 2021. **3**(3).
27. Furnas, C.C., *Flow of gases through beds of broken solids*. Vol. 307. 1929: US Government Printing Office.
28. De Larrard, F., *Concrete mixture proportioning: a scientific approach*. 1999: CRC Press.
29. Yu, A.B. and N. Standish, *A study of the packing of particles with a mixture size distribution*. Powder Technology, 1993. **76**(2): p. 113-124.
30. Mansoori, G.A., et al., *Equilibrium Thermodynamic Properties of the Mixture of Hard Spheres*. The Journal of Chemical Physics, 1971. **54**(4): p. 1523-1525.
31. Carnahan, N.F. and K.E. Starling, *Equation of State for Nonattracting Rigid Spheres*. The Journal of Chemical Physics, 1969. **51**(2): p. 635-636.
32. Yau, B.D.H.L., K.-Y. Chan, and D. Henderson, *Pair correlation functions for a hard sphere mixture in the colloidal limit*. Molecular Physics, 1997. **91**(6): p. 1137-1142.
33. Barrio, C. and J.R. Solana, *Consistency conditions and equation of state for additive hard-sphere fluid mixtures*. The Journal of Chemical Physics, 2000. **113**(22): p. 10180-10185.
34. Henderson, D. and K.-Y. Chan, *Solute-solvent pair distribution functions in highly asymmetric additive hard sphere mixtures*. The Journal of Chemical Physics, 1998. **108**(23): p. 9946-9947.
35. Henderson, D. and K.-Y. Chan, *Equation of state and correlation function contact values of a hard sphere mixture*. Molecular Physics, 2000. **98**(15): p. 1005-1010.
36. Yerazunis, S., S.W. Cornell, and B. Wintner, *Dense Random Packing of Binary Mixtures of Spheres*. Nature, 1965. **207**(4999): p. 835-837.
37. Wertheim, M.S., *Exact Solution of the Percus-Yevick Integral Equation for Hard Spheres*. Physical Review Letters, 1963. **10**(8): p. 321-323.
38. Gan, Y. and M. Kamlah, *Discrete element modelling of pebble beds: With application to uniaxial compression tests of ceramic breeder pebble beds*. Journal of the Mechanics and Physics of Solids, 2010. **58**(2): p. 129-144.
39. Gan, Y., M. Kamlah, and J. Reimann, *Computer simulation of packing structure in pebble beds*. Fusion Engineering and Design, 2010. **85**(10-12): p. 1782-1787.
40. Rissone, P., E.I. Corwin, and G. Parisi, *Long-Range Anomalous Decay of the Correlation in Jammed Packings*. Physical Review Letters, 2021. **127**(3).
41. Frenkel, D. and B. Smit, *Understanding molecular simulation: from algorithms to applications*. Vol. 1. 2001: Elsevier.
42. Sari, D. and A.G. Pasamehmetoglu, *The effects of gradation and admixture on the pumice lightweight aggregate concrete*. Cement and Concrete Research, 2005. **35**(5): p. 936-942.
43. Lu, X., et al., *3D microstructure design of lithium-ion battery electrodes assisted by X-ray nano-computed tomography and modelling*. Nature Communications, 2020. **11**(1).
44. Assouline, S., D. Tessier, and A. Bruand, *A conceptual model of the soil water retention*

- curve*. Water Resources Research, 1998. **34**(2): p. 223-231.
45. Lu, J., et al., *Root-induced changes of soil hydraulic properties – A review*. Journal of Hydrology, 2020. **589**: p. 125203.
 46. Luckham, P.F. and M.A. Ukeje, *Effect of particle size distribution on the rheology of dispersed systems*. Journal of colloid and interface science, 1999. **220**(2): p. 347-356.
 47. Yu, Y., et al., *Filtration performance of the granular bed filter used for industrial flue gas purification: A review of simulation and experiment*. Separation and Purification Technology, 2020. **251**: p. 117318.
 48. Hasnain, S.M., *Review on sustainable thermal energy storage technologies, Part I: heat storage materials and techniques*. Energy Conversion and Management, 1998. **39**(11): p. 1127-1138.
 49. Gautam, A. and R.P. Saini, *A review on technical, applications and economic aspect of packed bed solar thermal energy storage system*. Journal of Energy Storage, 2020. **27**: p. 101046.